ORIGINAL ARTICLE

High resolution heat stress over a Sahelian city: Present and future impact assessment and urban green effectiveness

Niels Souverijns[1*] | Koen De Ridder[1] | Sacha Takacs[1] | Nele Veldeman[1] | Marthe Michielsen[2] | Tomas Crols[1] | André K. Foamouhoue[3] | Godefroid Nshimirimana[3] | Ibrahim Dan Dijé[3] | Hassoumi Tidjani[4]

[1]Environmental Modeling Unit, Flemish Institute for Technological Research (VITO), Mol, Belgium

[2]Department of Earth and Environmental Sciences, KU Leuven, Leuven, Belgium

[3]African Centre of Meteorological Application for Development (ACMAD), Niamey, Niger

[4]Department of Environment, City of Niamey, Niamey, Niger

Correspondence
Niels Souverijns, Environmental Modeling Unit, Flemish Institute for Technological Research (VITO), Mol, Belgium
Email: niels.souverijns@vito.be

Funding information
ENABEL, Grant/Award Number: BEL170711-AP-05-21; Government of Flanders (Departement Omgeving), Grant/Award Number: IKF21/06

Cities in the Sahel are heavily impacted by heat stress. Climate change, growing population rates and urbanisation will increase the magnitude and intensity of urban heat stress towards the future. This study provides a comprehensive analysis of the current status of heat stress in Niamey (Niger) and future impacts by combining the results of two models operating at city-level: UrbClim which simulates (future) climate and GeoDynamiX, providing future city spatial extents combined with the results of a measurement campaign. Additionally, a meter-scale assessment of heat stress within the city is executed for a selection of city districts. Urban green and trees are effective mitigation tools for heat stress, which is observed in both measurements and model results, being most effective during the hottest hours of the day when they lower heat stress to less health-impacting levels. Future simulations show a strong increase in the spatial extent and intensity of extreme temperatures within the city. This impacts city dwellers, which will consequently experience much more days with extreme heat stress levels

towards the future, doubling or tripling depending on the climate scenario. Socio-economic impacts for mid-century are quantified, noting increases in heat-related mortality of several percentages compared to present-day values. Additionally, negative economic impacts of several percentages of the Gross Domestic Product are projected as heat stress will prohibit performing moderate or high-intensity activities during the hottest hours of the day, even in the shade.

KEYWORDS
Heat stress, Meter-scale, UrbClim, Niamey, Sahel, Urban Green, Climate change

1 | INTRODUCTION

Urbanisation ranks among the most significant manifestations of human impact on the environment. At the moment, cities are the home of 55 % of the world's population and this share is expected to increase sharply towards the future (Ritchie and Roser, 2018). Cities experience higher temperatures in comparison to their rural counterpart, which manifests most during the night, when temperature differences can be increasing up to 8 °C (Oke, 1982). This phenomenon is known as the 'Urban Heat Island' (UHI) and is mainly caused by the replacement of evaporative vegetation by areas with dense building materials and impervious surfaces with low albedo values. These surfaces absorb heat during the day and release it during the night (Oke, 1973; Lauwaet et al., 2015; Wouters et al., 2017). In the last decades, warming trends in cities are higher compared to rural counterparts (Liu et al., 2022) and climate change will continue to contribute to rising temperatures with more frequent, hotter and longer episodes of prolonged (extreme) heat (Perkins-Kirkpatrick and Lewis, 2020). For example, it is expected that cities will experience twice as much heat stress as rural areas towards the future (Wouters et al., 2017; Marcotullio et al., 2021). Of particular concern are Sahelian countries where an additional billion people will live in cities by 2050 compared to 2015 (OECD/SWAC, 2020; United Nations et al., 2022). These cities already experience high heat stress in present times (Oueslati et al., 2017) and the poor housing conditions (in dense informal settlements) that are often present also lead to enhanced heat exposure (Pasquini et al., 2020). In these countries, where the climate is rapidly warming and rapid urbanisation takes place, heat stress exposure is expected to increase by several magnitudes (Rohat et al., 2019).

Both urbanisation and climate change inevitably contribute to the burden of disease and premature deaths, particularly for vulnerable populations with limited adaptation resources (Kovats and Hajat, 2008; Li et al., 2015). Apart from the consequences on public health, excessive heat has a suite of environmental impacts such as decreasing water and air quality and stress on vegetation (Wilby, 2008; Whitehead et al., 2009; Hatfield and Prueger, 2015). These factors, in turn, affect human well-being and mortality (Kovats and Hajat, 2008; Vicedo-Cabrera et al., 2021; Marselle et al., 2020), energy consumption and public infrastructure (Santamouris et al., 2015; Ndiaye et al., 2017), violent incidents (Chersich et al., 2019) and labour productivity, which the latter is projected to decrease by several percentages of the worldwide Gross Domestic Product (GDP) (ILO, 2019; Zhao et al., 2021a). Furthermore, agriculture will be negatively affected, which is the backbone of the economy in most Sahel countries and underpinning livelihoods of a large share of the population (Sissoko et al., 2011).

To counter-effect the negative effects of excessive heat in cities, adaptive measures need to be taken. One of the most effective measures to create resilient cities is the implementation of blue and green urban infrastructure (e.g. Demuzere et al., 2014). The implementation of parks and large green infrastructure has shown to be an effective mitigation instrument for negative human health consequences (Bowler et al., 2010). Green infrastructure offers various mechanisms to cool the urban environment through evapotranspiration, increasing the albedo, providing shade and reducing the thermal load (Wong et al., 2021). Trees in particular provide effective urban heat mitigation tools, while treeless urban green spaces are overall less effective (Schwaab et al., 2021). While in developed regions, the mitigation potential of urban green has been studied thoroughly, limited studies have focused on the Sahel.

In order to analyse urban heat stress and the effect of adaptation and mitigation solutions, different approaches using several technologies have emerged. Most methods use thermal land surface temperature measurements derived from satellite data to map urban environments and their surroundings which, in turn, can be used to derive urban heat stress (e.g. Mallick et al., 2013; Zhou et al., 2019; Rodrigues de Almeida et al., 2021). Other studies such as Meier et al. (2017); Brousse et al. (2022) use a collection of atmospheric data retrieved from citizen weather stations. However, each approach has its disadvantages. Remote sensing data only allows for sub-kilometre resolution. In addition, the limited overpass frequency of satellites and cloudy conditions make it difficult to analyse the daily variability in heat stress and conduct future projections. The latter citizen-science approach, placing a sufficient amount of weather stations in the city is labour and cost-intensive and currently not feasible in developing countries in the Sahel. A valuable tool that overcomes all those problems are climate models as these provide high-resolution spatial and temporal information about heat stress patterns inside a city. Most studies of urban heat stress use sophisticated meso-scale models, having the advantage of providing a detailed physically-resolved representation of atmospheric dynamics, which can be used both for present-day and future studies. Yet, these coupled mesoscale–urban models have a high computational and time cost, which limits their application to kilometre-scale analyses (Kwok and Ng, 2021). Alternatively, micro-scale and building-scale models (e.g. Tominaga et al., 2015) offer very detailed representations of urban canopy and airflow, but are often limited to areas covering a few hundred meter (Mirzaei, 2015), which is not suitable for our study.

Therefore, in this study, we present the results of model simulations of the current climate for the city of Niamey (Niger) using respectively the UrbClim and High Resolution heat Exposure (HiREx) model. UrbClim produces meteorological information with a spatial resolution up to 100 m at a scale of urban agglomerations (De Ridder et al., 2015). Due to its fast run-time, it is well suited for simulations of several months to years. Moreover, UrbClim produces similar results as more sophisticated mesoscale models (García-Díez et al., 2016). The model has previously been validated in a variety of cities around the globe, yielding satisfactory results (Lauwaet et al., 2015; Zhou et al., 2016; Hooyberghs et al., 2019; Maheng et al., 2019; Sharma et al., 2019; Caluwaerts et al., 2020) and will also be evaluated here for the study area. This detailed climatology can subsequently be used as input for the HiREx meter-scale heat stress module, that is applied on three carefully selected districts in Niamey. To do so, the Wet Bulb Globe Temperature (WBGT), a widely applied index, was used to calculate/compute heat stress (Willett and Sherwood, 2012; Li et al., 2020). The heat stress maps were further used to analyse the cooling effects of urban greenery at district level as well as tree level. All model outcomes are validated by on-site heat stress measurements that have been executed. In a second step, both the climate change signal and future urbanisation (using the GeoDynamiX model (White et al., 2012, 2015; Crols et al., 2015; Crols, 2017)) will be taken into account to address the future impacts of heat stress.

The main goal of this study is to obtain spatially unprecedented (hundreds to 2 m spatial resolution) long-term present and future heat stress information for a region that is currently already experiencing episodes of extreme heat stress. Towards the future, population growth and climate change will contribute to even higher heat stress exposure, which will directly impact urban dwellers and the economy. The model results will therefore not only be used to obtain

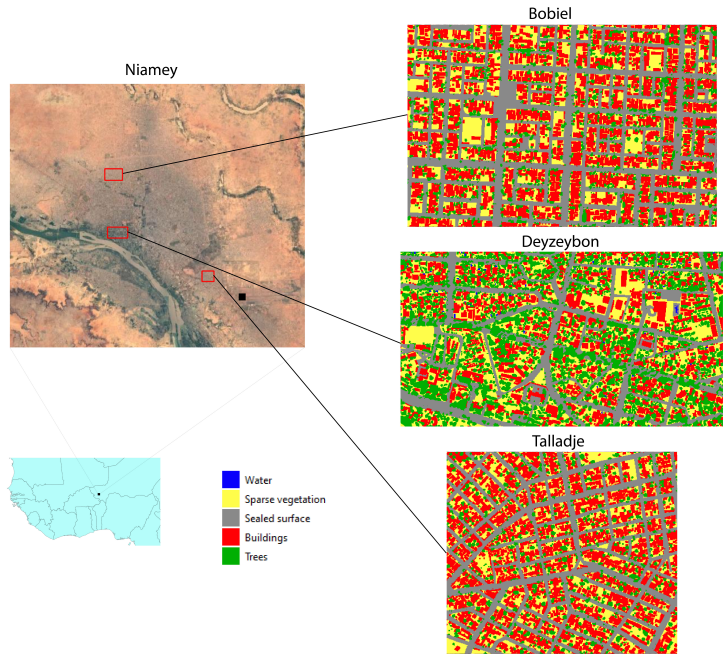

FIGURE 1 Location of Niamey in the Sahel region. The meter-scale heat stress modelling domains are indicated in red together with their respective land use. The black dot on the satellite image of Niamey indicates the location of the meteorological station that is used for evaluation purposes.

trustful climate information, but also to calculate present and future impacts on health and labour productivity, while providing hands-on information about the effectiveness of urban green as a mitigation practice that can directly be implemented in the region.

2 | MATERIALS AND METHODS

2.1 | Study Area

Niamey is part of the West Africa Sahel region and the capital of Niger. Its climate is characterised by year-round high temperatures and a brief rainy season from June until September. Monthly average temperatures are above 30 °C during the whole year and even rise above 40 °C in March, April and May, while night temperatures do not drop below 25 °C during these months (Sivakumar, 1986). Niamey's urban structure is characterised by a gradient ranging from both built-up and green areas in the city centre, which is located alongside the river banks, to more informal settlements with corrugated iron roofs and fewer green zones towards the periphery (Figure 1).

2.2 | GeoDynamiX urban growth model

Driven by high birth rates and rural exodus, the city of Niamey had a high population expansion since the mid 20th century, counting more than 1.3 million inhabitants today (United Nations et al., 2022). This rapid expansion resulted

in unstructured urbanisation and many informal settlements (Salamatou et al., 2015; Rossi and Dobigny, 2019, see also Figure 1).

We have simulated urban growth around Niamey with the GeoDynamiX model. This is an activity-based cellular automata (CA) land-use model. Next to land use, also population and employment can be computed for each cell, typically at a 100 m resolution (White et al., 2012, 2015; Vermeiren et al., 2022). Employment was not considered in this study due to a lack of spatial data. The main model drivers are distance-dependent transition rules of spatial attraction and repulsion, which reflect competition between activities or land uses at different scales from the local to the regional level. In most CA models these rules are limited to a local neighbourhood, while we consider the entire modelling area with logarithmic distances between cells. Travel times between cells in a transportation network can also be used (Crols et al., 2015), but this mode of the model was not chosen since the present road network of Niamey is still rather limited in comparison with the expected growth of the city in the coming decades. Next to the main transition rules, the model also takes physical suitability, zoning and accessibility into account. A full description of the model can be found in Crols (2017).

The model was calibrated using historical city extents and population data (2000-2018) obtained from the Global Human Settlement Layer (Corbane et al., 2018). The transition rules and model parameters were determined with semi-automated calibration based on the Covariance Matrix Adaptation Evolution Strategy (CMA-ES) algorithm of the DEAP library for Python (Fortin et al., 2012). Physical suitability values for urban growth were based on previous studies with the same model and were lower for steep slopes and (seasonal) water bodies. Slopes were calculated from SRTM digital elevation data of USGS (2018), while water bodies were taken from OpenStreetMap. Accessibility was computed towards the current road network and the Niger river. A full zoning map was not available, but urban green in the existing city and managed agriculture (from local maps) were excluded from urbanisation. The expected population growth and the trend of the urban share of population (Jones and O'Neill, 2016) were derived from three Shared Socioeconomic Pathways (SSP) scenarios (Fricko et al., 2017) of the IIASA database for Niger. These 3 scenarios are SSP2 (business-as-usual), SSP1 (sustainability) and SSP5 (fossil-fuelled development). The expected urban population for the region around Niamey in 2050 is actually similar in all these scenarios, growing to 9.5 million in 2050 (or 9.4 million in SSP5). In the SSP1 scenario we have reduced the additional urban area to host new people after 2018 by 10 % in comparison with SSP2 to simulate densification, while we have increased this additional urban area by 10 % in scenario SSP5 compared to SSP2 to simulate strong urban sprawl. In the zoning map of the SSP1 scenario plots of less managed agriculture were additionally added as protected zones.

2.3 | UrbClim urban climate model

UrbClim is an urban canopy model designed to simulate high spatial resolution climate variables at the scale of a city. The model is composed of a land surface scheme with simplified urban surface physics coupled to a 3D atmospheric boundary layer scheme. The 3D boundary layer model is tied at its lateral and top boundaries so that the synoptic forcing is properly considered. A detailed description of the land surface scheme can be found in De Ridder and Schayes (1997), whereas a complete description of the UrbClim model can be found in De Ridder et al. (2015).

The UrbClim modelling domain encompasses an area of 50 x 50 km that covers the whole city of Niamey. UrbClim simulations were executed at a spatial resolution of 200 m for a period of 20 years representing the last decades (2001-2020). This unprecedented spatial scale allows to take into account the impact of the urban canopy on temperatures and heat stress, which is currently omitted by most state-of-the art reanalyses and climate models that perform long-term simulations. To validate the results of the Urbclim model, data from a weather station near the airport of Niamey is used (denoted by a black dot in Figure 1). This weather station is recognised by the World Meteorological Organization

Climate scenario	Local Δ°C	Urban growth scenario	Future population
RCP2.6	1.03	SSP1	9.5M
RCP4.5	1.36	SSP5	9.4M
RCP8.5	1.88	SSP2	9.5M

TABLE 1 Future simulations executed for 2041-2060. Representative Concentration Pathways (RCPs) from CORDEX-AFRICA for the climate change signal are combined with Shared Socioeconomic Pathways (SSPs) for urban growth projections. Relative average difference in temperature with respect to 2000-2020 are denoted together with future population amounts (reference population 2020: 1.3M).

and follows its standards. Unfortunately, it is the only long-term available dataset that allowed us to compare the maximal daily temperature (Tmax) and the daily minimal temperature (Tmin) with the modelled air temperature from UrbClim.

To conduct the UrbClim simulation for the desired study area, certain data sets are required as input. For the boundary conditions of the 3D atmospheric model, the ERA-5 reanalysis data set from the European Centre for Medium Range-Weather Forecasting (Hersbach et al., 2020) is used. This dataset has a 31 km resolution that is updated on an hourly basis. Anthropogenic heat flux is derived, at 30 arc-seconds resolution maps, from Jin et al. (2019). Besides meteorological and anthropogenic heat flux data, a detailed representation of land surface properties is required as input. The land cover map is derived from the Copernicus Global Land Cover Layers at 100 m resolution (Buchhorn et al., 2020). This dataset is combined with built-up data from the Global Human Settlement layer (Corbane et al., 2021). For each grid cell, the percentage of urban land cover is obtained from the global 30 m resolution impervious surface map (Zhang et al., 2020). Maps of vegetation cover fraction were derived, at 30 m resolution, from existing NDVI maps constructed from Landsat 8 images, available on the Google Earth Engine (Gorelick et al., 2017). The NDVI maps were converted into vegetation cover fractions using a linear relationship proposed by Gutman and Ignatov (1998). Lastly, terrain elevation data was taken from the Copernicus GLO-30 DEM dataset, which is freely available at a global scale (ESA, 2020).

Three future simulations are executed for the period 2041-2060 by combining the results of the urban growth model (Section 2.2) and the climate change signal from a selection of models from the CORDEX-AFRICA project (Table 1). A list of the regional climate models that were selected based on recommendations from Bichet et al. (2020); Dosio et al. (2021) can be found in the Supporting Information (Table S1). Instead of re-running the UrbClim model with each of the ensemble CORDEX-AFRICA models as input, a quantile mapping bias algorithm is used to perturb the historical time series data from the UrbClim numerical model following the climate change signal of these models (Olsson et al., 2009; Willems and Vrac, 2011). A detailed description of the procedure applied in this study can be found in Lauwaet et al. (2019, Chapter 4). Apart from the meteorological climate change signal, also the land surface input datasets were adapted to the new city extents as projected in section 2.2. Future anthropogenic heat fluxes, as projected by Jin et al. (2019) for 2050 were also included.

2.4 | High Resolution heat Exposure (HiREx) model

Out of the different heat stress indicators that exist, WBGT is nowadays the most utilised index (Budd, 2008). This index uses standard meteorological variables and can be calculated both in direct solar radiation and shaded conditions (Lauwaet et al., 2020). In this study, the calculation of the outdoor WBGT follows the methodology of Liljegren et al. (2008), based on recommendations in a review paper by Lemke and Kjellstrom (2012), and is further indicated as the

Category	Maximum physical activity	Wet Bulb Globe Temperature limit for persons acclimatised to heat (°C)
Extreme heat stress	Resting (115W)	33
Very high heat stress	Low activity (180W)	30
High heat stress	Moderate activity (300W)	28
Moderate heat stress	Intense activity (415W)	26
Low heat stress	Very intense activity (520W)	25

TABLE 2 Wet Bulb Globe Temperature reference values for acclimatised for five classes of metabolic rate categorised into heat stress levels (ISO, 2017). A detailed description and examples of the levels of metabolic rate can be found in ISO (2017, Annex E)

High Resolution heat Exposure (HiREx) model. The following formula provides the outdoor WBGT as a weighted sum of the natural wet bulb temperature (T_w), the black globe temperature (T_g) and the dry bulb (ambient) temperature (T_a) (Eq. 1).

$$WBGT = 0.7T_w + 0.2T_g + 0.1T_a \quad (1)$$

The WBGT value gives an indication for the average heat stress exposure of a human being. The limits for acclimatised persons (which we assume to be valid for a large part of the population living in Niamey) are based on ISO (2017) and listed in Table 2.

The meteorological input data that is required for the HiREx model is achieved from the UrbClim simulations at 200 m executed over the city (i.e. hourly 2 m air temperature, relative humidity, wind speed and land surface temperature). The use of this spatially detailed input data allows to take into account the impact of the urban canopy and the urban heat island on heat stress. This information is omitted in previous studies using large-scale climate models or reanalyses. Next to this, surface pressure, shortwave and longwave radiation are taken from the ERA-5 reanalysis data set. The model is executed at very high spatial resolution (2 m), allowing to investigate local differences in heat stress and the impact of (individual) tree canopy. As such, a detailed representation of land surface is needed, including individual buildings and trees. While such detailed information is often available in city administrations of developed countries, no such data currently exist for the city of Niamey. Hence, manual digitisation was conducted for three selected city districts: (i) Bobiel, (ii) Deyzeybon, (iii) Talladje (Figure 1). These three city districts were chosen due to their different spatial structure. The districts of Bobiel and Talladje are characterised by a dense road network, compact low-rise buildings and widely spaced, individual trees. The urban morphology of Deyzeybon differs from the former two. Its road network is less dense, the buildings are mostly high-rise consisting of single-standing houses, offices or hotels. The remaining space is for a considerable part occupied by grouped trees. Based on Google Earth and Open Street Map, these neighbourhoods were digitised and classified in QGIS into five land cover classes. Building and tree heights were estimated at respectively 6 m and 9 m for Bobiel and Talladje and 13 m and 16 m for Deyzeybon. The resulting digitised land cover maps have a spatial resolution of 2 m and are shown for each district (Figure 1). A table accounting for the relative occurrence of each land cover class can be found in the Supporting Information (Table S2). By taking into account the solar zenith and azimuth angles, shaded areas cast by buildings or trees were calculated for each hour of the year, as also the sky view factor (the fraction of the sky hemisphere visible from the ground; Dirksen et al., 2019). Combining the meteorological data with the detailed land surface properties, the HiREx

(a) Sun

(b) Shade

FIGURE 2 Heat stress data logger setup.

module is able to iteratively calculate the WBGT at a 2 m resolution for the three city districts, taking into account shade and solar zenith angles in each model time step.

2.5 | Measurement campaign + validation

For each district, three campaigns on three different days in May 2022 were executed under the supervision of the African Centre of Meteorological Application for Development (ACMAD), focusing on performing WGBT measurements. All measurements were executed by local community participants. Practices on how to involve and engage the local community in measurement campaigns and generate awareness for climate change research are described in Souverijns et al. (2022). The main goal of these campaigns were two-fold. One the one hand, we wanted to provide reference validation data for the HiREx model. Secondly, quantitative evidence of the cooling impact of vegetation in the city of Niamey was aimed for. Each of the three monitoring campaigns involved 6 portable data loggers of the type WBGT-2010SD, the specification of which are available from `https://www.atal.nl/media/downloads/mn/az/AT-HTS01.pdf`. These loggers measure T_g, T_a and the relative humidity, which can be converted to T_w and, in its turn, be used to calculate WBGT (see Eq. 1).

Each individual measurement campaign was conducted in pairs, one of the devices measuring in the shade of a tree and the other receiving full solar radiation exposure at a nearby position (meters to tens of meters away; Figure 2). Each mounted on a tripod such that the meteorological components were measured at a height of about 1.5 m above the surface level. Each pair of data loggers was set up at a designated location. Pictures of each setup were taken that include location information (GPS latitude and longitude). On each of the campaign days, each WBGT data logger was used to conduct measurements between 9:00 AM and 5:00 PM. As a result of the three campaign days, each involving 6 WBGT data loggers (at three different locations), a total of 144 hourly data points were collected. An overview of the locations of the data loggers and their respective measurements are visualised and in `https://vitobelgium.github.io/niamey-foret-climatique` and can be downloaded therewith.

2.6 | Socio-Economic impacts

Heat stress in cities has considerable impacts on its residents as stated in Section 1. The socio-economic impact of present and future heat stress is quantified by calculating three different indicators, namely, (i) lost working hours (LWH), (ii) gross domestic product (GDP) per capita (%) and (iii) relative risk of mortality (%), which are detailed below. The high-resolution WBGT analysis at 2 m spatial resolution, including the UrbClim 200 m results as input data, will reveal an unprecedented level of detail in the heat stress impact analysis, not only considering the urban canopy effects, but also (individual) buildings and tree effects and therefore also detailed street morphology, which will be considered in the analysis of the results.

Based on ISO-standards, the number of LWH per year can be calculated based on the WBGT for the different city districts (ISO, 2017). For moderate activities (300W; see Table 2), the fraction of each working hour that is lost is calculated as (the formulas for different intensities of activities can be found in the Supporting Information):

$$LWH = 1 - \begin{cases} 1; & WBGT < 31.0 \\ -0.5 * WBGT + 16.5; & 31.0 \leq WBGT \leq 33.0 \\ 0 & WBGT > 33.0; \end{cases} \quad (2)$$

LWHs caused by heat stress affects economic output and therefore also the GDP. This was calculated based on the global non-linear relationship between annual average temperature and change in the gross domestic product (GDP) per capita developed by Burke et al. (2015). In that research, the empirical model foundation (based on GDP data from 1960 to 2010) shows evidence that economic activity in all regions is coupled with the global climate. Based on their relation, an average and a high estimation of GDP decrease per capita was calculated for Niamey denoting the impact of the change in average temperatures over the full modelling domain between the mid-century projections (2041-2060) and present times (2001-2020). The average estimation is calculated using the global empirical formula (Eq. 1 in the Supporting Information), while the high estimation is taken from countries showing similar average annual temperatures such as Mali (Eq. 2 in the Supporting Information).

Next to economic impacts, heat stress causes health-related incidents and also affects mortality. The increase in relative risk of mortality (%) is defined as the probability of mortality increase when a population group is exposed to warmer temperatures than normal. The model applied in this study is based on the quantification of the temperature–mortality function, which is assumed to be V-shaped. The temperature value at which mortality is the lowest is defined as the optimum temperature, which we took as the 80^{th} percentile of the average daily temperature based on WHO (2014); Gasparrini et al. (2015); Takahashi et al. (2007). For temperatures above this point, the relative risk of mortality increases in a linear way depending on the heat-related mortality numbers of the country. While the majority of studies related to heat-related mortality are for urban populations in Europe, America, and China, there is very limited to no information on temperature–mortality functions populations in Africa such as Niger. Therefore, to be as objective as possible, we calculated a minimal, an average, and a maximal increase in relative risk of mortality per degree increase in temperature based on results found in global studies of respectively 6 %, 10 % and 20 % (Zhao et al., 2021b; Gasparrini et al., 2015).

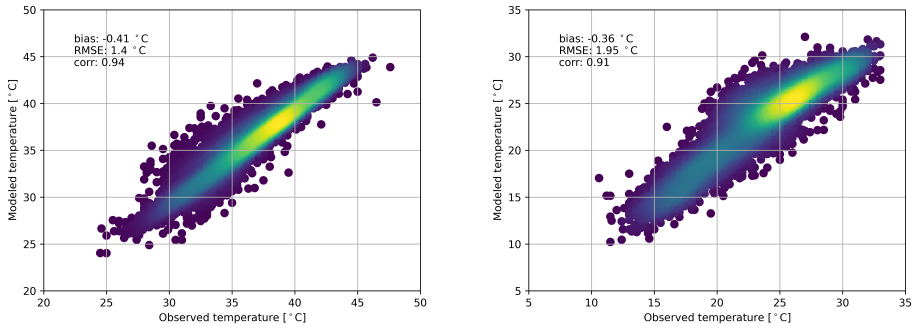

(a) Maximum daily temperature

(b) Minimum daily temperature

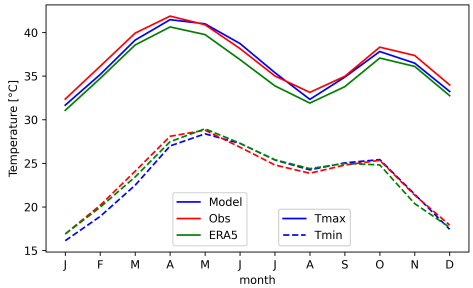

(c) Average monthly temperature

FIGURE 3 Evaluation of UrbClim results for the period 2001-2020 compared to WMO station measurements at the airport (its location is depicted by a dot in Figure 1). ERA-5 results are added in Figure 3c.

3 | RESULTS

3.1 | Model validation

Meteorological data from the last two decades were retrieved from the weather station at the airport of Niamey (located at the black dot in Figure 1) and compared to the UrbClim model. The results show a close relationship for the maximal daily temperature (Tmax), with a correlation of 0.94 between modelled and retrieved data (Figure 3a). Similarly, a correlation of 0.91 was found for the minimal daily temperature (Tmin, Figure 3b). In both cases (maximal daily temperature and minimal daily temperature), the Urbclim model tends to underestimate Tmax and Tmin with respectively a bias of -0.41 °C and -0.39 °C. This underestimation is particularly noticeable for the first months of the year, from January until April (Figure 3c). In the rest of the year (from April to December), observed and modelled temperatures are aligned to each other. Furthermore, a root mean square error (RMSE) of 1.95 and 1.41 was found for Tmin and Tmax respectively. UrbClim outperforms ERA-5 when simulating day-time temperatures, while slightly lower performance is found for night-time temperatures.

For the meter-scale heat stress validation, a total of 144 measurements were captured during the three campaigns, with a wide range of WBGT values varying from around 25 °C (low heat stress) to 34 °C (extreme heat stress, Figure 4). A correlation of 0.66 was calculated between the modelled and retrieved WBGT. A -0.15 °C bias was calculated, showing limited structural differences of heat stress in the HiREx model compared to the observations. For each

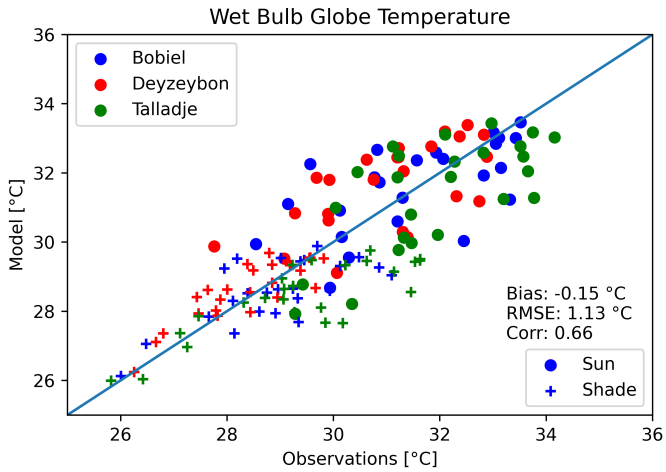

FIGURE 4 Comparison between modelled Wet Bulb Globe Temperature values from the HiREx model and local measurements obtained from three campaign days.

location, two clusters of measurements can be detected: one cluster with lower WBGT identified as the measurements that were obtained in the shade, and one cluster with higher WBGT showing the measurements impacted by direct solar radiation. This distinction is well captured in the model attaining similar offsets compared to the measurements. The added value of using UrbClim as model input for the HiREx model instead of directly using ERA-5 is demonstrated in the Supporting Information (Figure S1 & Table S3).

3.2 | Urban Green impact

March-April-May are the months attaining the highest temperatures in Niamey (Figure 3c). The average heat stress during this period at noon for each district is visualised for the year 2020 (Figure 5). Due to the high spatial resolution, the urban structure of Bobiel, Deyzeybon and Talladje can easily be recognised on these maps (compare with Figure 1). At all three neighbourhoods, the street network and open sealed surfaces are the hot spots attaining very high heat stress. In all neighbourhoods, a clear distinction between shaded areas and areas with direct radiation of the sun can be noticed, as shaded areas attain values that are at least one heat stress category lower. The density of trees has a strong effect on the amount of heat stress. Bobiel and Talladje mainly have individual trees, while Deyzeybon has larger concentrations of grouped trees. The latter lowers heat stress up to two categories, to moderate levels (Figure 5).

The cooling effect of trees on heat stress is even clearer in the results of the measurement campaigns that have been executed in the different city districts. Results for the 19$^{\text{th}}$ of May 2022 show that shaded areas attain heat stress levels that are up to two categories lower compared to areas with direct sunlight exposure (Figure 6). When comparing Deyzeybon with Bobiel and Talladje, differences in heat stress are most noticeable in the early afternoon. During that time, the more vegetated district of Deyzeybon is constantly one heat stress category lower than the two other areas (Figure 6). Results for the other two measurement campaign days can be found in the Supporting Information (Figure S2).

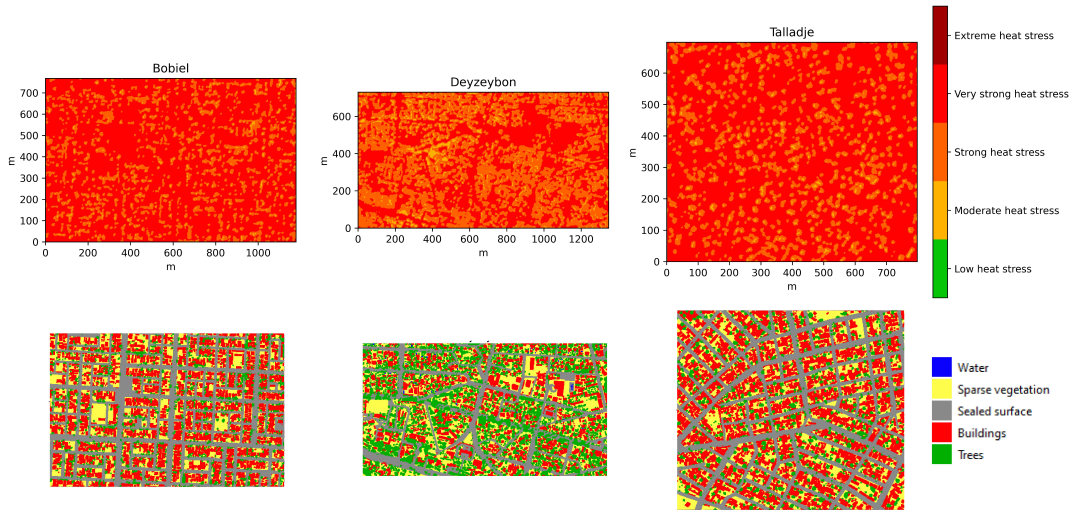

FIGURE 5 Average heat stress in the three city districts during March-April-May 2020 at noon simulated by the HiREx model. Land use maps for the three regions are depicted. Comparing both, a clear pattern of lower heat stress is found in areas with higher tree cover densities.

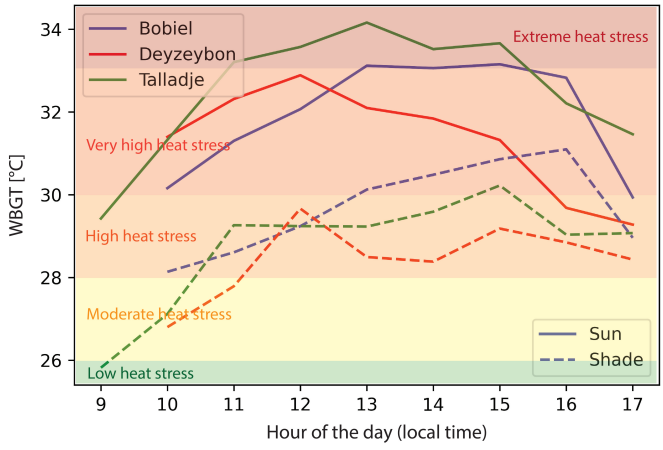

FIGURE 6 Wet Bulb Globe Temperature measurements for three locations in the three selected districts in the sun and shade on 19-05-2022.

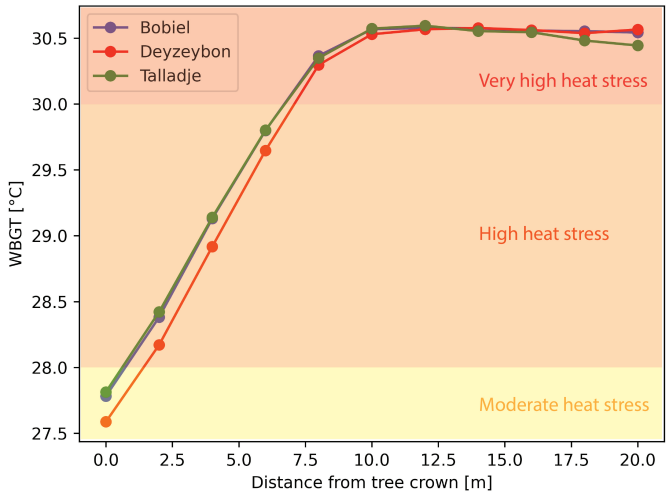

FIGURE 7 Cooling effect of trees at noon during March-April-May (highest solar zenith angle) with respect to the distance of the tree crown for three city districts in Niamey based on HiREx model results.

Concerning the spatial cooling effects of trees, during peak heat of the day at noon (when shadows are limited to areas directly beneath the tree crown due to the high solar zenith angle), a clear influence on heat stress is visible up to 10m from the tree crown (Figure 7). This again shows the extensive cooling potential of trees, lowering WBGT up to 3 °C and two heat stress categories, clearly mitigating the very high and extreme heat danger that is present during the hottest hours of the day.

3.3 | City Growth

All SSP scenarios indicate a massive population growth in Niger and its urban areas. The population of Niamey would become more than 4 times larger during the simulated time period (2018-2050) of this study, reaching almost 10 million inhabitants. Consequently, the size of the urban area will have a similar exponential growth if no thorough planning and densification are organised by the government. The urban land use in the study area has expanded from 10,626 ha to 20,850 ha during the calibration period (2000-2018). The simulation results project a further growth by 2050 to 87,537 ha (SSP1), 94,006 ha (SSP2, Figure 8) or 100,916 ha (SSP5). The city would mainly develop towards the north and the east in a rather concentric and continuous pattern as hardly any restrictions, roads or main villages are present. The southern bank of the Niger river is much more hilly and has as such lower values for urban suitability.

3.4 | Future climate impacts

Mid-century projections of future climate impacts on Niamey are provided. A number of climate indicators are calculated for both present and future time periods. These are included in a viewer that is freely accessible allowing users to detect the impact of climate change and urban expansion on the city (`https://uclip.marvin.vito.be/uclip`). Furthermore, all maps can be analysed and downloaded. One example indicator is visualised in this paper (Figure 9),

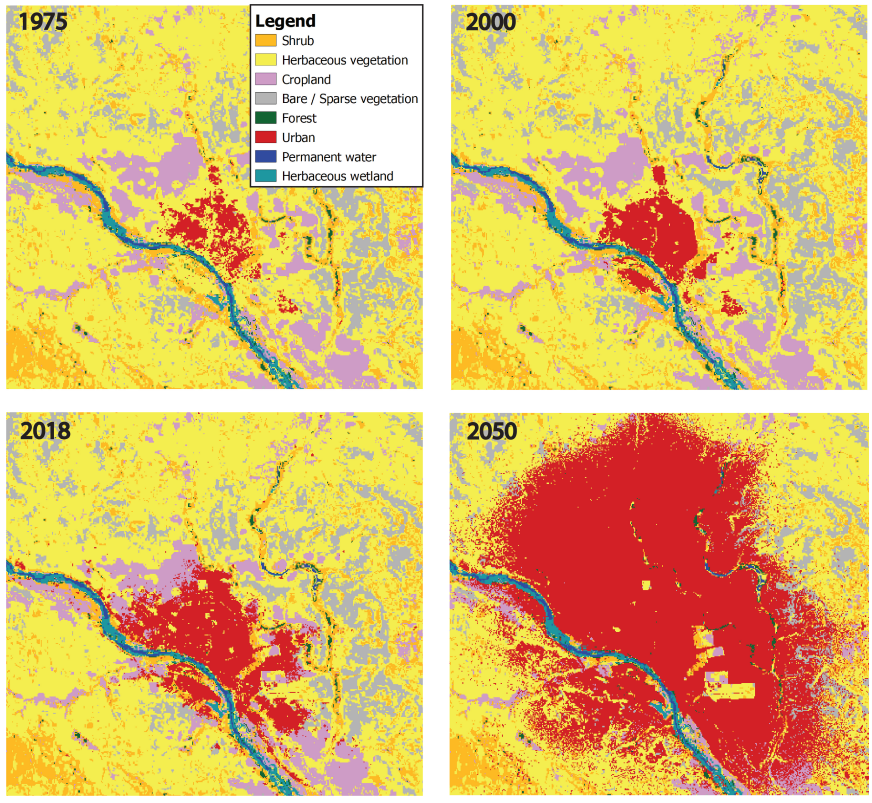

FIGURE 8 Historical evolution of the city and projection for 2050 based on the SSP2 scenario using the GeoDynamiX model.

showing the number of heatwave days. A heatwave is defined when both daily minimum and maximum temperatures are greater than the 90^{th} percentile for three or more consecutive days, calculated on present-day temperature climatology (Faye et al., 2021). For present-days, heat waves occur mostly within the city limits, averaging about 15 days per year. Towards the future, this increases sharply in each of the three scenarios. Even in a low-emission scenario (RCP2.6), the number of heatwave days within the city bounds doubles to 30. In the high-emission scenario (RCP8.5), this three-folds, increasing the amount of heat stress on the inhabitants considerably.

This is also reflected in the future heat stress simulations over the three districts (Figure 10). In present times, extreme heat stress (WBGT > 33 °C) only occurs for a limited amount of hours in the hottest months of the year and only when exposed to direct sunlight. In the shade of trees, one would almost never experience extreme heat stress. This changes towards the future. At first, the hours during the day and the number of days in which people will be exposed to extreme heat will increase sharply compared to present-day, even in the lowest emission scenario. Furthermore, a worrying trend can be seen that also during several hours per year, extreme heat stress will be experienced in the shade (dashed boxplots). In the high-emission scenario (RCP8.5), both Bobiel and Talladje will experience these heat stress values. Only Deyzeybon, which has much more vegetation, will provide enough extensive patches of trees in which extreme heat stress is mitigated.

These increases in heat stress towards mid-century have socio-economic consequences for the city dwellers. As expected, the number of LWHs for moderate activities increases for all scenarios, similar to the amount of heat stress. In the high-emission scenario the number of LWHs almost doubles, both in the shade and the sun (excluding rooftops), going up to 2000 hours in the sun and 1000 hours in the shade (Figure 11). This will have a profound effect on productivity and economic activities in the region. The impacts on intense activities is even higher, and corresponding figures (together with light activities) can be found in the Supporting Information.

For the average estimation of the GDP decrease per capita, the results show a decrease of 2 to 3.5 % depending on the climate scenario by 2050. When taking the high estimation approach, the decrease is even more accentuated reaching values up to 4.5 - 9 % depending on the climate scenario (Figure 12a). The results also show an increase in mortality rates in the city due to heat. In the city of Niamey, it will increase by several percentages towards mid-century, from 1.5 to 2.5 % in an average estimation about 3 to 5 % in a high estimation, depending on the emission scenario (Figure 12b).

4 | DISCUSSION AND CONCLUSION

Heat stress is a major problem with large socio-economic consequences. However, up to now, detailed mitigation and impact studies have not been performed in the Sahelian region. In this study, both a measurement campaign and a modelling approach were adopted to analyse heat stress and the thermal comfort for the city of Niamey (Niger) for present and future conditions. The main advantage of using the UrbClim model for these analyses lies in its fast runtime. Compared to more sophisticated and computationally intensive models, we omit calculating the pressure gradient, but use the prescribed large-scale forcing from ERA-5. As such, thermal circulation systems, such as sea breezes and katabatic winds are not calculated in UrbClim. Despite this, several previous validation experiments have been executed showing the capability of UrbClim in simulating standard meteorological quantities such as energy fluxes, wind speeds and temperatures (Lauwaet et al., 2015; Zhou et al., 2016; Hooyberghs et al., 2019; Maheng et al., 2019; Sharma et al., 2019; Caluwaerts et al., 2020), including over African cities (Souverijns et al., 2022).

Despite the limited availability of validation data over Niamey, we also executed a validation exercise here. Our 200 m modelling framework provides reliable results when compared with the data retrieved from the single long-

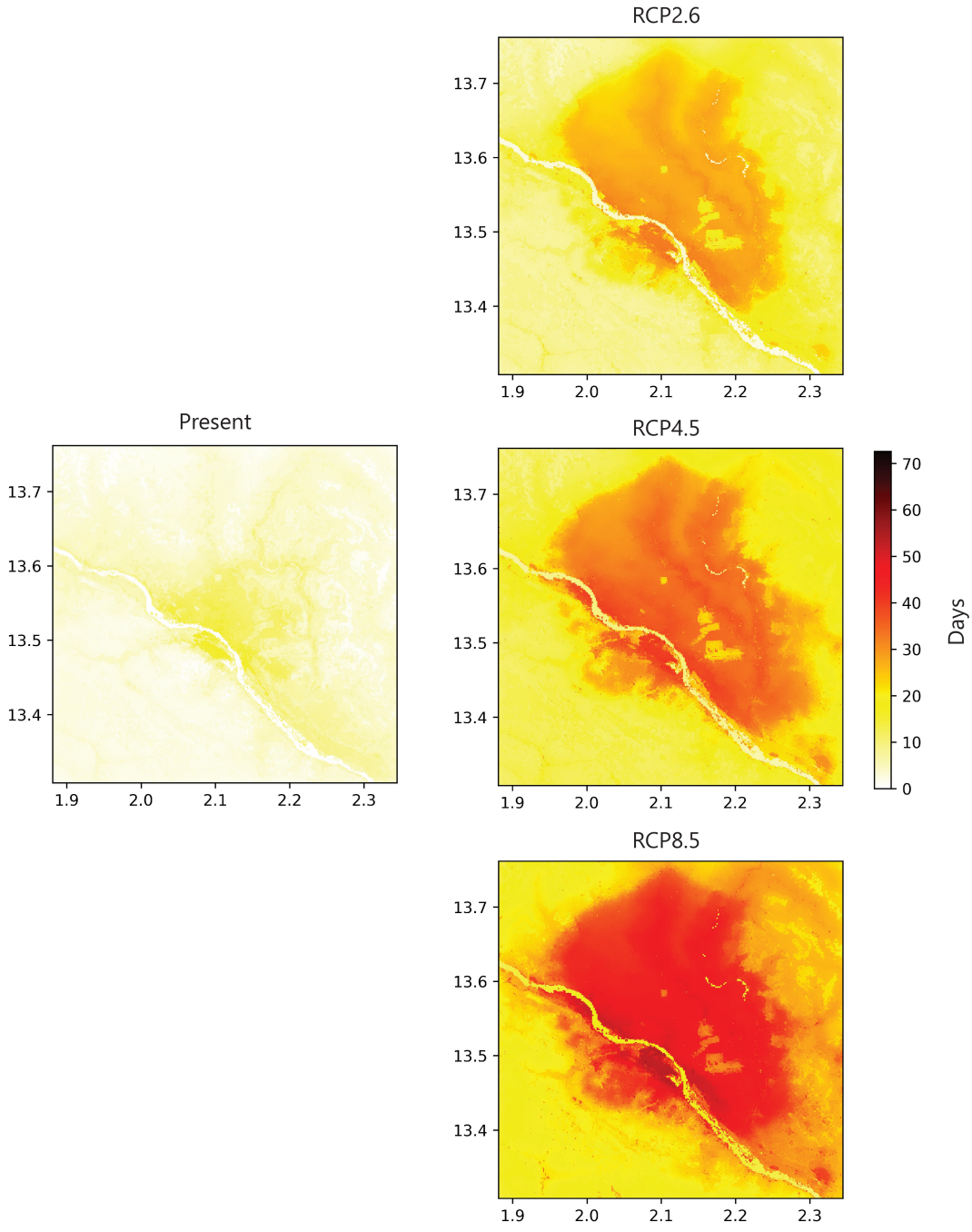

FIGURE 9 Number of heatwave days per year over Niamey in a present (2001-2020) and future scenarios (2041-2060) taking into account both the effects of climate change (RCP scenarios) and population increases (SSP scenarios; see also Figure 8). These scenarios are detailed in Table 1.

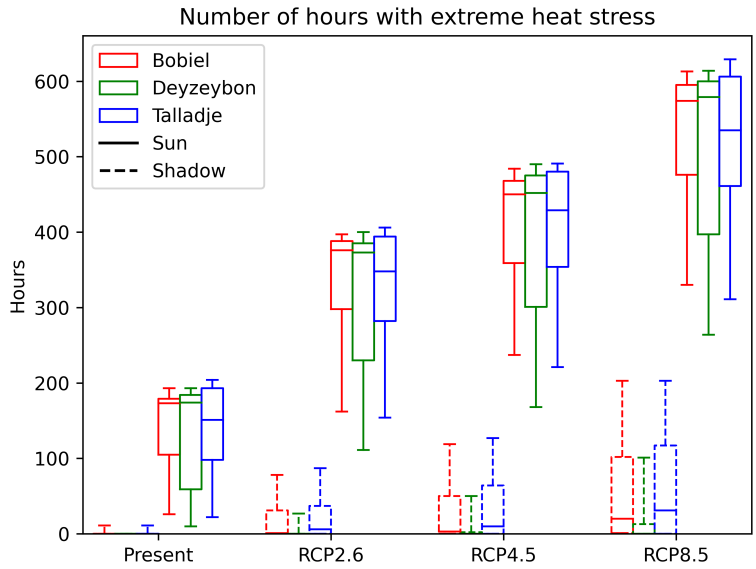

FIGURE 10 Number of hours per year with extreme heat stress for present (2001-2020) and future scenarios (2041-2060).

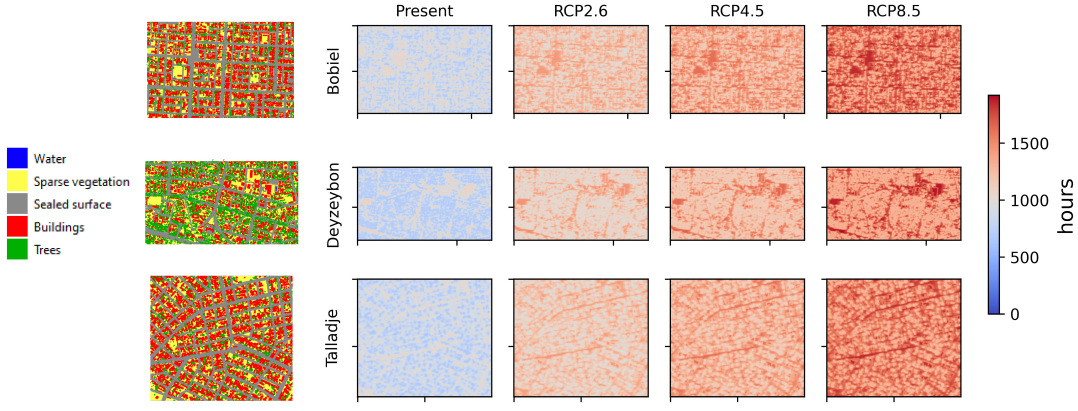

FIGURE 11 Number of lost working hours (LWH) per year for moderate activities for present (2001-2020) and future scenarios (2041-2060). Land use maps for the three districts depicted are added for clarity. A clear increase in LWH is visible in each scenario, almost doubling (light blue to red) for the RCP8.5 scenario by 2041-2060.

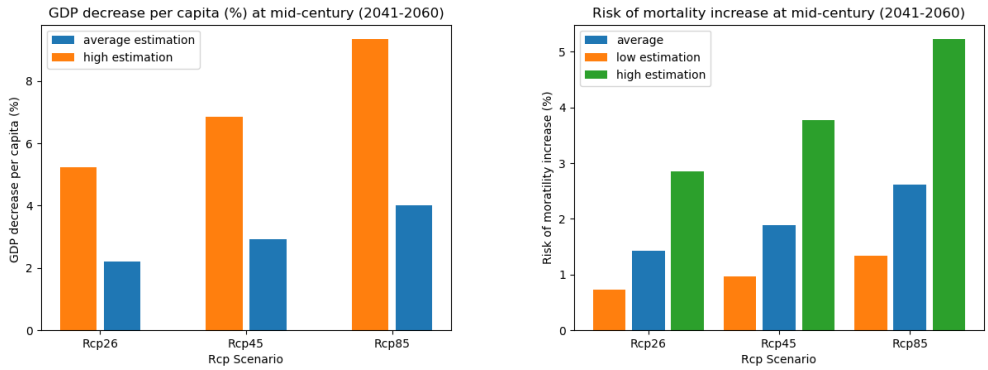

(a) Gross Domestic Product (b) Mortality

FIGURE 12 Socio-economic impacts of climate change in the city of Niamey in future scenarios (2041-2060).

term weather station in the region. Compared to ERA-5, better results are achieved for day-time, while a slightly lower accuracy is obtained during the night. It must be noted that this weather station is located outside of the city, experiencing limited influence of the urban canopy. The added accuracy of UrbClim in city areas is greatest within city premises, where higher temperatures are simulated caused by the UHI effect (see e.g. Figure 9), which is not considered in other large-scale models or reanalyses, such as ERA-5. Previous validation exercises over Africa, such as in Souverijns et al. (2022), put confidence in the results produced by UrbClim over Niamey.

As air temperature alone is not sufficient when studying thermal comfort, the HiREx model, calculating the outdoor WBGT at 2 m scale resolution was used to investigate heat stress. The results of this model were compared to the measurements retrieved from three measurement campaigns and showed a good relationship with a slight underestimation of the model for the highest heat stress levels. Part of this discrepancy might be attributed to erroneous humidity measurements, losing accuracy at very high temperatures and radiation levels. The data loggers used during the campaigns did not have any type of shielding, making them susceptible to any change in humidity by for example wind (Tarara and Hoheisel, 2007; Botero-Valencia et al., 2022).

The construction of heat stress maps at meter-scale resolution for three different districts in the city of Niamey allowed to discover relationships between local heat stress, land cover and urban vegetation. A first conclusion that can be drawn is that thermal comfort in Niamey improves with increased availability of urban green. This was noticeable when comparing Deyzeybon (which has higher densities of urban trees) with Bobiel and Talladje. We ascribe the lower heat stress in Deyzeybon to the fact that trees cover more than 30 % of the surface area and often occur in patches while in Bobiel and Talladje, trees are often single-standing, accounting for only 11 % of the area. In general, trees account for a decrease in heat stress of 3 °C in WBGT (often two heat stress categories), as confirmed by the measurements. These results are in line with previous studies in mid-latitudes. For instance, Lauwaet et al. (2020) stated that for the city of Ghent (Belgium) on a hot summer day, building and tree shades provide a cooling effect of respectively around 2 °C and 3 °C in WBGT. Other related studies in Israel and Europe reported that overhead shading reduces thermal stress, with respectively more cooling provided by trees than by a shading mesh (Shashua-Bar et al., 2011; Schwaab et al., 2021). The cooling effects of urban greenery have already been studied in different ways and under different settings (Ng et al., 2012; Coccolo et al., 2016; Zheng et al., 2016). However, finding the best urban configuration to reduce heat stress is often difficult as it is highly context dependent. For instance, the amount of local

heat absorption depends on the solar altitude, street geometry and surface reflectance of city components. Climate conditions as well as tree species can also play a role in reducing heat stress (Jamei et al., 2016; Wong et al., 2021). Hence it is crucial to get more insights about which trees and climatic conditions have the optimal effects in their particular city to advise policymakers and urban designers, certainly in vulnerable regions such as the Sahel.

Climate change and urbanisation will affect living conditions in the city of Niamey. Results show that heat stress exposure will increase substantially due to increases in temperature (extremes), but also the growth of the city population and increased spatial extent simulated by the GeoDynamiX model show severe expansions of the amount of people that will be affected. Two- to three-fold increases in the frequency of heatwaves and extreme heat stress are expected depending on the scenario. Remarkable is that even in the low emission scenario (RCP2.6), a substantial increase in the number of heatwaves and hours with extreme heat stress is observed, which was already observed in previous work (Kjellstrom et al., 2018). This increase can partly be explained by the strong growth in population of the city by 2050, which will increase UHI intensities even at low levels of climate change. A strong relation between UHI intensity and city size and compactness is present (Oke, 1973; Zhou et al., 2017).

This increase in heat (stress) towards the future has shown to have implications on the productivity of workers and is reflected in the number of lost working hours, increasing sharply towards the future. Shifting working hours to the morning and evening is only partly possible, as daylight is often required to perform activities for the lowest incomes, severely restricting their time of activity. The ISO-based formula used in this study to calculate lost working hours is characterised by sharp boundaries in which efficiency drops relatively fast with increased WBGT values (i.e. between 31 °C and 33 °C). Some studies based on empirical data suggest a smoother increase in lost working hours with decreases in efficiency already occurring at WBGT values of 20 °C, while physical activities can continue up to 40 °C (Foster et al., 2021). More studies are needed to fine-tune these relationships and to take into account the adaptation capacity of local citizens, which might be acclimatised to higher WBGT values.

It is without saying that this will have a profound impact on work and income of this part of the population. As a result, a substantial loss in GDP is projected for the city of Niamey, ranging from 2 - 4 % by mid-century. These results are in line with the recent International Monetary Fund report for Sub-Saharan Africa, that calculated a 2.2 % decrease per 1 °C increase, resulting in 2.4 - 4.2 % when adapting this rate for future temperatures of Niamey (Maino and Emrullahu, 2022). The rate of 2.2 °C per 1 °C has been calculated based on all Sub-Saharan data. This could in reality be higher for fragile states with a hot climate such as Niger, supporting our high estimation results of GDP decrease. It must be noted that the values obtained for Niamey are higher than the global average, which is below 2 % (Borg et al., 2021), showing the vulnerability of the region towards extreme heat stress.

Apart from economic consequences, health risks are also associated with extreme heat. The increase in the number of hours with (extreme) heat limits the amount of activity that a person can perform. When this is ignored, health risks can occur, which is not limited to the elderly and weak. This is reflected in the projection of mortality numbers, which will increase towards mid-century by about 1.5 - 2.5 % in an average estimation. These results are in line with other studies, where increases of 0.5 - 2 % per 1 °C are found (Abatan et al., 2016; Lim et al., 2015). Kapwata et al. (2022) even calculated a 4 % increase towards the mid-century, supporting the high estimation of mortality increase obtained in this research. In Niamey, this might be even higher, as a lot of people are suffering from under-nutrition and bad health care. This accounts for a population of 10 million people to an additional 1200 to 2000 deaths on an annual basis.

The approach presented in this contribution is associated with a number of methodological challenges. The main problem encountered was the lack of data for Niamey. High resolution land cover and height maps are needed to calculate meter-scale heat stress maps, which were not available. This is why, in this study, we were forced to manually digitise three neighbourhoods in order to perform meter-scale heat stress modelling. Apart from detailed information,

the amount of reference weather stations was lacking for validation. For this study, only one weather station with valid temperature data was found near the airport of Niamey. This weather station is not the most representative to compare urban heat stress as it is placed in an area with a low building density and a more open spatial structure compared to other places of the city. Besides, the only measured climatic data was temperature whereas other climatic variables such as humidity and wind speed were not captured. This constrains our comparison and understanding of local context to only two parameters out of several others. Further, the impact calculation study is based on existing relationships. Detailed impact curve calculations again require detailed information on population statistics and mortality, which is not available, limiting the detail of this study. Despite these limitations, a framework that can be replicated to different locations and contexts is provided. We therefore hope our study will trigger additional future research to further explore urban heat stress in the region and continue to find and implement different mitigation strategies with respect to heat stress. Urban configuration, differences between tree types and building material characteristics are aspects that provide interesting incentives for policy makers and urban planners. In order to achieve this, it is of crucial importance to have access to more (detailed) regional data to better understand local initiatives and challenges. Citizens in the Sahel could for example provide a crucial role in performing meteorological measurements, creating capacity building and involvement in local heat stress adaptation and mitigation plans.

Author Contributions

Niels Souverijns: Conceptualization; Data curation; Formal analysis; Investigation; Methodology; Software; Validation; Visualisation; Writing. **Koen De Ridder**: Conceptualization; Funding acquisition; Methodology; Project administration; Supervision; Writing. **Sacha Takacs**: Conceptualization; Data curation; Formal analysis; Investigation; Methodology; Software; Visualisation; Writing. **Nele Veldeman**: Project administration; Supervision; Writing. **Marthe Michielsen**: Data curation; Formal analysis; Software; Visualisation; Writing. **Tomas Crols**: Data curation; Formal analysis; Software; Visualisation; Writing. **André K. Foamouhoue**: Conceptualization; Funding acquisition; Supervision; Writing. **Godefroid Nshimirimana**: Data curation; Resources; Writing. **Ibrahim Dan Dijé**: Data curation; Resources; Writing. **Hassoumi Tidjani**: Data curation; Resources; Supervision; Writing.

Acknowledgements

We would like to thank the different members of the community in Niamey that assisted in executing the measurement campaign. The dashboard which allows consultation of all indicators, including download options can be accessed via `https://uclip.marvin.vito.be/`. Daily temperature data for present and future over Niamey can be accessed via `https://doi.org/10.5281/zenodo.6674705`. All Wet Bulb Globe Temperature measurements are visualised in `https://vitobelgium.github.io/niamey-foret-climatique` and can be downloaded as raw csv files therewith. We would also like to thank Joseph Kaunda for assisting in urban growth modelling during his student internship at VITO. Two anonymous reviewers are thanked for their comments that significantly improved this manuscript. This project is funded by the Belgian federal government through the Wehubit program implemented by Enabel (BEL170711-AP-05-21) and by the Government of Flanders through the G-STIC Climate Action Programme (IKF 21/06).

Conflict of interest

The authors declare no conflicts of interest

references

Abatan, A. A., Abiodun, B. J., Lawal, K. A. and Gutowski Jr, W. J. (2016) Trends in extreme temperature over nigeria from percentile-based threshold indices. *International Journal of Climatology*, **36**, 2527–2540.

Bichet, A., Diedhiou, A., Hingray, B., Evin, G., Touré, N. E., Browne, K. N. A. and Kouadio, K. (2020) Assessing uncertainties in the regional projections of precipitation in CORDEX-AFRICA. *Climatic Change*, **162**, 583–601. URL: https://link.springer.com/10.1007/s10584-020-02833-z.

Borg, M. A., Xiang, J., Anikeeva, O., Pisaniello, D., Hansen, A., Zander, K., Dear, K., Sim, M. R. and Bi, P. (2021) Occupational heat stress and economic burden: A review of global evidence. *Environmental Research*, **195**, 110781. URL: https://doi.org/10.1016/j.envres.2021.110781https://linkinghub.elsevier.com/retrieve/pii/S001393512100075X.

Botero-Valencia, J., Mejia-Herrera, M. and Pearce, J. M. (2022) Design and implementation of 3-D printed radiation shields for environmental sensors. *HardwareX*, **11**, e00267. URL: https://doi.org/10.1016/j.ohx.2022.e00267.

Bowler, D. E., Buyung-Ali, L., Knight, T. M. and Pullin, A. S. (2010) Urban greening to cool towns and cities: A systematic review of the empirical evidence. *Landscape and Urban Planning*, **97**, 147–155. URL: http://dx.doi.org/10.1016/j.landurbplan.2010.05.006.

Brousse, O., Simpson, C., Walker, N., Fenner, D., Meier, F., Taylor, J. and Heaviside, C. (2022) Evidence of horizontal urban heat advection in London using 6 years of data from a citizen weather station network. *Environmental Research Letters*. URL: https://iopscience.iop.org/article/10.1088/1748-9326/ac5c0f.

Buchhorn, M., Lesiv, M., Tsendbazar, N.-E., Herold, M., Bertels, L. and Smets, B. (2020) Copernicus Global Land Cover Layers—Collection 2. *Remote Sensing*, **12**, 1044. URL: https://www.mdpi.com/2072-4292/12/6/1044.

Budd, G. M. (2008) Wet-bulb globe temperature (WBGT)—its history and its limitations. *Journal of Science and Medicine in Sport*, **11**, 20–32. URL: https://linkinghub.elsevier.com/retrieve/pii/S1440244007001478.

Burke, M., Hsiang, S. M. and Miguel, E. (2015) Global non-linear effect of temperature on economic production. *Nature*, **527**, 235–239.

Caluwaerts, S., Hamdi, R., Top, S., Lauwaet, D., Berckmans, J., Degrauwe, D., Dejonghe, H., De Ridder, K., De Troch, R., Duchêne, F., Maiheu, B., Van Ginderachter, M., Verdonck, M. L., Vergauwen, T., Wauters, G. and Termonia, P. (2020) The urban climate of Ghent, Belgium: A case study combining a high-accuracy monitoring network with numerical simulations. *Urban Climate*, **31**, 100565. URL: https://doi.org/10.1016/j.uclim.2019.100565.

Chersich, M. F., Swift, C. P., Edelstein, I., Breetzke, G., Scorgie, F., Schutte, F. and Wright, C. Y. (2019) Violence in hot weather: Will climate change exacerbate rates of violence in South Africa? *South African Medical Journal*, **109**, 447–449.

Coccolo, S., Kämpf, J., Scartezzini, J. L. and Pearlmutter, D. (2016) Outdoor human comfort and thermal stress: A comprehensive review on models and standards. *Urban Climate*, **18**, 33–57. URL: http://dx.doi.org/10.1016/j.uclim.2016.08.004.

Corbane, C., Florczyk, A., Pesaresi, M., Politis, P. and Syrris, V. (2018) GHS built-up grid, derived from Landsat, multitemporal (1975-1990-2000-2014), R2018A.

Corbane, C., Syrris, V., Sabo, F., Politis, P., Melchiorri, M., Pesaresi, M., Soille, P. and Kemper, T. (2021) Convolutional neural networks for global human settlements mapping from Sentinel-2 satellite imagery. *Neural Computing and Applications*, **33**, 6697–6720. URL: https://doi.org/10.1007/s00521-020-05449-7https://link.springer.com/10.1007/s00521-020-05449-7.

Crols, T. (2017) *Integrating network distances into an activity based cellular automata land-use model. Semi-automated calibration and application to Flanders, Belgium*. Ph.D. thesis, Vrije Universiteit Brussel and VITO. URL: https://geodynamix.eu/sites/geodynamix/files/PhD_thesis_Tomas_Crols_Fin.pdf.

Crols, T., White, R., Uljee, I., Engelen, G., Poelmans, L. and Canters, F. (2015) A travel time-based variable grid approach for an activity-based cellular automata model. *International Journal of Geographical Information Science*, **29**, 1757–1781.

De Ridder, K., Lauwaet, D. and Maiheu, B. (2015) UrbClim - A fast urban boundary layer climate model. *Urban Climate*, **12**, 21–48.

De Ridder, K. and Schayes, G. (1997) The IAGL land surface model. *Journal of Applied Meteorology*, **36**, 167–182.

Demuzere, M., Orru, K., Heidrich, O., Olazabal, E., Geneletti, D. and Orru, H. (2014) Mitigating and adapting to climate change : Multi-functional and multi-scale assessment of green urban infrastructure. *Journal of Environmental Management*, **146**, 107–115.

Dirksen, M., Ronda, R. J., Theeuwes, N. E. and Pagani, G. A. (2019) Sky view factor calculations and its application in urban heat island studies. *Urban Climate*, **30**, 100498. URL: https://doi.org/10.1016/j.uclim.2019.100498.

Dosio, A., Jury, M. W., Almazroui, M., Ashfaq, M., Diallo, I., Engelbrecht, F. A., Klutse, N. A. B., Lennard, C., Pinto, I., Sylla, M. B. and Tamoffo, A. T. (2021) Projected future daily characteristics of African precipitation based on global (CMIP5, CMIP6) and regional (CORDEX, CORDEX-CORE) climate models. *Climate Dynamics*, **57**, 3135–3158. URL: https://doi.org/10.1007/s00382-021-05859-whttps://link.springer.com/10.1007/s00382-021-05859-w.

ESA (2020) Copernicus DEM - Global and European Digital Elevation Model (COP-DEM).

Faye, M., Dème, A., Diongue, A. K. and Diouf, I. (2021) Impact of different heat wave definitions on daily mortality in Bandafassi, Senegal. *PLoS ONE*, **16**, e0249199. URL: https://dx.plos.org/10.1371/journal.pone.0249199.

Fortin, F.-A., De Rainville, F.-M., Gardner, M.-A., Parizeau, M. and Gagné, C. (2012) DEAP: Evolutionary Algorithms Made Easy . *Journal of Machine Learning Research*, **13**, 2171–2175.

Foster, J., Smallcombe, J. W., Hodder, S., Jay, O., Flouris, A. D., Nybo, L. and Havenith, G. (2021) An advanced empirical model for quantifying the impact of heat and climate change on human physical work capacity. *International Journal of Biometeorology*, **65**, 1215–1229.

Fricko, O., Havlik, P., Rogelj, J., Klimont, Z., Gusti, M., Johnson, N., Kolp, P., Strubegger, M., Valin, H., Amann, M., Ermolieva, T., Forsell, N., Herrero, M., Heyes, C., Kindermann, G., Krey, V., McCollum, D. L., Obersteiner, M., Pachauri, S., Rao, S., Schmid, E., Schoepp, W. and Riahi, K. (2017) The marker quantification of the Shared Socioeconomic Pathway 2: A middle-of-the-road scenario for the 21st century. *Global Environmental Change*, **42**, 251–267. URL: https://www.sciencedirect.com/science/article/pii/S0959378016300784.

García-Díez, M., Lauwaet, D., Hooyberghs, H., Ballester, J., De Ridder, K. and Rodó, X. (2016) Advantages of using a fast urban boundary layer model as compared to a full mesoscale model to simulate the urban heat island of Barcelona. *Geoscientific Model Development*, **9**, 4439–4450. URL: https://gmd.copernicus.org/articles/9/4439/2016/.

Gasparrini, A., Guo, Y., Hashizume, M., Lavigne, E., Zanobetti, A., Schwartz, J., Tobias, A., Tong, S., Rocklöv, J., Forsberg, B. et al. (2015) Mortality risk attributable to high and low ambient temperature: a multicountry observational study. *The lancet*, **386**, 369–375.

Gorelick, N., Hancher, M., Dixon, M., Ilyushchenko, S., Thau, D. and Moore, R. (2017) Google Earth Engine: Planetary-scale geospatial analysis for everyone. *Remote Sensing of Environment*, **202**, 18–27.

Gutman, G. and Ignatov, A. (1998) The derivation of the green vegetation fraction from NOAA/AVHRR data for use in numerical weather prediction models. *International Journal of Remote Sensing*, **19**, 1533–1543. URL: https://www.tandfonline.com/doi/full/10.1080/014311698215333.

Hatfield, J. L. and Prueger, J. H. (2015) Temperature extremes: Effect on plant growth and development. *Weather and Climate Extremes*, **10**, 4–10. URL: https://linkinghub.elsevier.com/retrieve/pii/S2212094715300116.

Hersbach, H., Bell, B., Berrisford, P., Hirahara, S., Horányi, A., Muñoz-Sabater, J., Nicolas, J., Peubey, C., Radu, R., Schepers, D., Simmons, A., Soci, C., Abdalla, S., Abellan, X., Balsamo, G., Bechtold, P., Biavati, G., Bidlot, J., Bonavita, M., Chiara, G., Dahlgren, P., Dee, D., Diamantakis, M., Dragani, R., Flemming, J., Forbes, R., Fuentes, M., Geer, A., Haimberger, L., Healy, S., Hogan, R. J., Hólm, E., Janisková, M., Keeley, S., Laloyaux, P., Lopez, P., Lupu, C., Radnoti, G., Rosnay, P., Rozum, I., Vamborg, F., Villaume, S. and Thépaut, J. (2020) The ERA5 global reanalysis. *Quarterly Journal of the Royal Meteorological Society*, **146**, 1999–2049. URL: https://onlinelibrary.wiley.com/doi/10.1002/qj.3803.

Hooyberghs, H., Berckmans, J., Lauwaet, D., Lefebre, F. and De Ridder, K. (2019) Climate variables for cities in Europe from 2008 to 2017.

ILO (2019) *Working on a warmer planet: the imact of heat stress on labour productivity and decent work*. Geneva, Switzerland: International Labour Office.

ISO (2017) ISO 7243: Ergonomics of the thermal environment — Assessment of heat stress using the WBGT (wet bulb globe temperature) index.

Jamei, E., Rajagopalan, P., Seyedmahmoudian, M. and Jamei, Y. (2016) Review on the impact of urban geometry and pedestrian level greening on outdoor thermal comfort. *Renewable and Sustainable Energy Reviews*, **54**, 1002–1017. URL: http://dx.doi.org/10.1016/j.rser.2015.10.104.

Jin, K., Wang, F., Chen, D., Liu, H., Ding, W. and Shi, S. (2019) A new global gridded anthropogenic heat flux dataset with high spatial resolution and long-term time series. *Scientific Data*, **6**, 139. URL: http://dx.doi.org/10.1038/s41597-019-0143-1http://www.nature.com/articles/s41597-019-0143-1.

Jones, B. and O'Neill, B. C. (2016) Spatially explicit global population scenarios consistent with the Shared Socioeconomic Pathways. *Environmental Research Letters*, **11**, 084003.

Kapwata, T., Gebreslasie, M. T. and Wright, C. Y. (2022) An analysis of past and future heatwaves based on a heat-associated mortality threshold: towards a heat health warning system. *Environmental health*, **21**, 1–12.

Kjellstrom, T., Freyberg, C., Lemke, B., Otto, M. and Briggs, D. (2018) Estimating population heat exposure and impacts on working people in conjunction with climate change. *International Journal of Biometeorology*, **62**, 291–306.

Kovats, R. S. and Hajat, S. (2008) Heat Stress and Public Health: A Critical Review. *Annual Review of Public Health*, **29**, 41–55. URL: https://www.annualreviews.org/doi/10.1146/annurev.publhealth.29.020907.090843.

Kwok, Y. T. and Ng, E. Y. Y. (2021) Trends, topics, and lessons learnt from real case studies using mesoscale atmospheric models for urban climate applications in 2000–2019. *Urban Climate*, **36**, 100785. URL: https://doi.org/10.1016/j.uclim.2021.100785https://linkinghub.elsevier.com/retrieve/pii/S2212095521000158.

Lauwaet, D., Hooyberghs, H., Lefebre, F., De Ridder, K., Veldeman, N. and Willems, P. (2019) Climate-fit.city: Urban climate data for demonstration cases, Deliverable 5.2. *Tech. rep.*, VITO. URL: https://project.climate-fit.city/wp-content/uploads/2020/07/D5.2-Urban-Climate-Data-For-Demonstration-Cases.pdf.

Lauwaet, D., Hooyberghs, H., Maiheu, B., Lefebvre, W., Driesen, G., Van Looy, S. and De Ridder, K. (2015) Detailed urban heat island projections for cities worldwide: Dynamical downscaling CMIP5 global climate models. *Climate*, **3**, 391–415.

Lauwaet, D., Maiheu, B., De Ridder, K., Boënne, W., Hooyberghs, H., Demuzere, M. and Verdonck, M.-L. (2020) A New Method to Assess Fine-Scale Outdoor Thermal Comfort for Urban Agglomerations. *Climate*, **8**, 6. URL: https://www.mdpi.com/2225-1154/8/1/6.

Lemke, B. and Kjellstrom, T. (2012) Calculating Workplace WBGT from Meteorological Data: A Tool for Climate Change Assessment. *Industrial Health*, **50**, 267–278.

Li, D., Yuan, J. and Kopp, R. E. (2020) Escalating global exposure to compound heat-humidity extremes with warming. *Environmental Research Letters*, **15**, 064003. URL: https://iopscience.iop.org/article/10.1088/1748-9326/ab7d04.

Li, M., Gu, S., Bi, P., Yang, J. and Liu, Q. (2015) Heat Waves and Morbidity: Current Knowledge and Further Direction-A Comprehensive Literature Review. *International Journal of Environmental Research and Public Health*, **12**, 5256–5283. URL: http://www.mdpi.com/1660-4601/12/5/5256.

Liljegren, J. C., Carhart, R. A., Lawday, P., Tschopp, S. and Sharp, R. (2008) Modeling the wet bulb globe temperature using standard meteorological measurements. *Journal of Occupational and Environmental Hygiene*, **5**, 645–655.

Lim, Y.-H., Reid, C. E., Mann, J. K., Jerrett, M. and Kim, H. (2015) Diurnal temperature range and short-term mortality in large us communities. *International journal of biometeorology*, **59**, 1311–1319.

Liu, Z., Zhan, W., Bechtel, B., Voogt, J., Lai, J., Chakraborty, T., Wang, Z.-h., Li, M., Huang, F. and Lee, X. (2022) Surface warming in global cities is substantially more rapid than in rural background areas. *Communications Earth & Environment*, **3**, 219. URL: https://www.nature.com/articles/s43247-022-00539-x.

Maheng, D., Ducton, I., Lauwaet, D., Zevenbergen, C. and Pathirana, A. (2019) The Sensitivity of Urban Heat Island to Urban Green Space—A Model-Based Study of City of Colombo, Sri Lanka. *Atmosphere*, **10**, 151. URL: https://www.mdpi.com/2073-4433/10/3/151.

Maino, R. and Emrullahu, D. (2022) Climate change in sub-saharan africa's fragile states. *IMF Working Papers*, WP/22/54.

Mallick, J., Rahman, A. and Singh, C. K. (2013) Modeling urban heat islands in heterogeneous land surface and its correlation with impervious surface area by using night-time ASTER satellite data in highly urbanizing city, Delhi-India. *Advances in Space Research*, **52**, 639–655. URL: http://dx.doi.org/10.1016/j.asr.2013.04.025https://linkinghub.elsevier.com/retrieve/pii/S0273117713002536.

Marcotullio, P. J., Keßler, C. and Fekete, B. M. (2021) The future urban heat-wave challenge in Africa: Exploratory analysis. *Global Environmental Change*, **66**, 102190. URL: https://linkinghub.elsevier.com/retrieve/pii/S0959378020307731.

Marselle, M. R., Bowler, D. E., Watzema, J., Eichenberg, D., Kirsten, T. and Bonn, A. (2020) Urban street tree biodiversity and antidepressant prescriptions. *Scientific Reports*, **10**, 22445. URL: https://doi.org/10.1038/s41598-020-79924-5http://www.nature.com/articles/s41598-020-79924-5.

Meier, F., Fenner, D., Grassmann, T., Otto, M. and Scherer, D. (2017) Crowdsourcing air temperature from citizen weather stations for urban climate research. *Urban Climate*, **19**, 170–191. URL: https://linkinghub.elsevier.com/retrieve/pii/S2212095517300068.

Mirzaei, P. A. (2015) Recent challenges in modeling of urban heat island. *Sustainable Cities and Society*, **19**, 200–206. URL: http://dx.doi.org/10.1016/j.scs.2015.04.001https://linkinghub.elsevier.com/retrieve/pii/S2210670715000414.

Ndiaye, A., Adamou, R., Gueye, M. and Diedhiou, A. (2017) Global Warming and Heat Waves in West-Africa: Impacts on Electricity Consumption in Dakar (Senegal) and Niamey (Niger). *International Journal of Energy and Environmental Science*, **2**, 16–26. URL: http://www.sciencepublishinggroup.com/j/ijees.

Ng, E., Chen, L., Wang, Y. and Yuan, C. (2012) A study on the cooling effects of greening in a high-density city: An experience from Hong Kong. *Building and Environment*, **47**, 256–271.

OECD/SWAC (2020) Africa's Urbanisation Dynamics 2020: Africapolis, Mapping a New Urban Geography. *Tech. rep.*, OECD Publishing, Paris.

Oke, T. (1973) City size and the urban heat island. *Atmospheric Environment (1967)*, **7**, 769–779. URL: https://www.sciencemag.org/lookup/doi/10.1126/science.147.3660.920-ahttps://linkinghub.elsevier.com/retrieve/pii/0004698173901406.

Oke, T. R. (1982) The energetic basis of the urban heat island. *Quarterly Journal of the Royal Meteorological Society*, **108**, 1–24. URL: https://onlinelibrary.wiley.com/doi/10.1002/qj.49710845502.

Olsson, J., Berggren, K., Olofsson, M. and Viklander, M. (2009) Applying climate model precipitation scenarios for urban hydrological assessment: A case study in Kalmar City, Sweden. *Atmospheric Research*, **92**, 364–375. URL: http://dx.doi.org/10.1016/j.atmosres.2009.01.015https://linkinghub.elsevier.com/retrieve/pii/S0169809509000325.

Oueslati, B., Pohl, B., Moron, V., Rome, S. and Janicot, S. (2017) Characterization of Heat Waves in the Sahel and Associated Physical Mechanisms. *Journal of Climate*, **30**, 3095–3115. URL: https://journals.ametsoc.org/doi/10.1175/JCLI-D-16-0432.1.

Pasquini, L., van Aardenne, L., Godsmark, C. N., Lee, J. and Jack, C. (2020) Emerging climate change-related public health challenges in Africa: A case study of the heat-health vulnerability of informal settlement residents in Dar es Salaam, Tanzania. *Science of the Total Environment*, **747**, 141355. URL: https://doi.org/10.1016/j.scitotenv.2020.141355.

Perkins-Kirkpatrick, S. E. and Lewis, S. C. (2020) Increasing trends in regional heatwaves. *Nature Communications*, **11**, 3357. URL: http://dx.doi.org/10.1038/s41467-020-16970-7http://www.nature.com/articles/s41467-020-16970-7.

Ritchie, H. and Roser, M. (2018) Urbanization. URL: https://ourworldindata.org/urbanization.

Rodrigues de Almeida, C., Teodoro, A. C. and Gonçalves, A. (2021) Study of the Urban Heat Island (UHI) Using Remote Sensing Data/Techniques: A Systematic Review. *Environments*, **8**, 105. URL: https://www.mdpi.com/2076-3298/8/10/105.

Rohat, G., Flacke, J., Dosio, A., Dao, H. and Maarseveen, M. (2019) Projections of Human Exposure to Dangerous Heat in African Cities Under Multiple Socioeconomic and Climate Scenarios. *Earth's Future*, **7**, 528–546. URL: https://doi.org/10.1029/2018EF001020https://onlinelibrary.wiley.com/doi/10.1029/2018EF001020.

Rossi, J.-P. and Dobigny, G. (2019) Urban Landscape Structure of a Fast-Growing African City: The Case of Niamey (Niger). *Urban Science*, **3**, 63.

Salamatou, A. I., Abdoulaye, D., Boubacar, M. M., Abou Soufianou, S., Ali, M. and Mahamane, S. (2015) Dynamics of a third world city: Case of Niamey, Niger. *Journal of Geography and Regional Planning*, **8**, 120–130.

Santamouris, M., Cartalis, C., Synnefa, A. and Kolokotsa, D. (2015) On the impact of urban heat island and global warming on the power demand and electricity consumption of buildings - A review. *Energy and Buildings*, **98**, 119–124. URL: http://dx.doi.org/10.1016/j.enbuild.2014.09.052.

Schwaab, J., Meier, R., Mussetti, G., Seneviratne, S., Bürgi, C. and Davin, E. L. (2021) The role of urban trees in reducing land surface temperatures in European cities. *Nature Communications*, **12**, 1–11.

Sharma, R., Hooyberghs, H., Lauwaet, D. and De Ridder, K. (2019) Urban Heat Island and Future Climate Change—Implications for Delhi's Heat. *Journal of Urban Health*, **96**, 235–251. URL: http://link.springer.com/10.1007/s11524-018-0322-y.

Shashua-Bar, L., Pearlmutter, D. and Erell, E. (2011) The influence of trees and grass on outdoor thermal comfort in a hot-arid environment. *International Journal of Climatology*, **31**, 1498–1506.

Sissoko, K., van Keulen, H., Verhagen, J., Tekken, V. and Battaglini, A. (2011) Agriculture, livelihoods and climate change in the West African Sahel. *Regional Environmental Change*, **11**, 119–125. URL: http://link.springer.com/10.1007/s10113-010-0164-y.

Sivakumar, M. V. (1986) Climate of Niamey. *Tech. rep.*, International Crops Research Institute for the Semi-Arid Tropics (ICRISAT).

Souverijns, N., De Ridder, K., Veldeman, N., Lefebre, F., Kusambiza-Kiingi, F., Memela, W. and Jones, N. K. (2022) Urban heat in Johannesburg and Ekurhuleni, South Africa: A meter-scale assessment and vulnerability analysis. *Urban Climate*, **46**, 101331. URL: https://doi.org/10.1016/j.uclim.2022.101331https://linkinghub.elsevier.com/retrieve/pii/S2212095522002498.

Takahashi, K., Honda, Y. and Emori, S. (2007) Assessing mortality risk from heat stress due to global warming. *Journal of risk research*, **10**, 339–354.

Tarara, J. M. and Hoheisel, G.-A. (2007) Low-cost Shielding to Minimize Radiation Errors of Temperature Sensors in the Field. *HortScience*, **42**, 1372–1379.

Tominaga, Y., Akabayashi, S.-i., Kitahara, T. and Arinami, Y. (2015) Air flow around isolated gable-roof buildings with different roof pitches: Wind tunnel experiments and CFD simulations. *Building and Environment*, **84**, 204–213. URL: http://dx.doi.org/10.1016/j.buildenv.2014.11.012https://linkinghub.elsevier.com/retrieve/pii/S0360132314003655.

United Nations, Department of Economic and Social Affairs and Population Division (2022) *World Population Prospects 2022: Summary of Results*. New York: United Nations. URL: https://www.un.org/development/desa/pd/sites/www.un.org.development.desa.pd/files/undesa_pd_2022_wpp_key-messages.pdf.

USGS (2018) USGS EROS Archive - Digital Elevation - Shuttle Radar Topography Mission (SRTM) 1 Arc-Second Global. URL: https://doi.org/10.5066/F7PR7TFT.

Vermeiren, K., Crols, T., Uljee, I., De Nocker, L., Beckx, C., Pisman, A., Broekx, S. and Poelmans, L. (2022) Modelling urban sprawl and assessing its costs in the planning process: A case study in Flanders, Belgium. *Land Use Policy*, **113**, 105902.

Vicedo-Cabrera, A. M., Scovronick, N., Sera, F., Royé, D., Schneider, R., Tobias, A., Astrom, C., Guo, Y., Honda, Y., Hondula, D. M., Abrutzky, R., Tong, S., Coelho, M. d. S. Z. S., Saldiva, P. H., Lavigne, E., Correa, P. M., Ortega, N. V., Kan, H., Osorio, S., Kyselý, J., Urban, A., Orru, H., Indermitte, E., Jaakkola, J. J., Ryti, N., Pascal, M., Schneider, A., Katsouyanni, K., Samoli, E., Mayvaneh, F., Entezari, A., Goodman, P., Zeka, A., Michelozzi, P., De'Donato, F., Hashizume, M., Alahmad, B., Diaz, M. H., Valencia, C. D. L. C., Overcenco, A., Houthuijs, D., Ameling, C., Rao, S., Di Ruscio, F., Carrasco-Escobar, G., Seposo, X., Silva, S., Madureira, J., Holobaca, I. H., Fratianni, S., Acquaotta, F., Kim, H., Lee, W., Iniguez, C., Forsberg, B., Ragettli, M. S., Guo, Y. L., Chen, B. Y., Li, S., Armstrong, B., Aleman, A., Zanobetti, A., Schwartz, J., Dang, T. N., Dung, D. V., Gillett, N., Haines, A., Mengel, M., Huber, V. and Gasparrini, A. (2021) The burden of heat-related mortality attributable to recent human-induced climate change. *Nature Climate Change*, **11**, 492–500.

White, R., Engelen, G. and Uljee, I. (2015) *Modeling cities and regions as complex systems: From theory to planning applications*. MIT Press.

White, R., Uljee, I. and Engelen, G. (2012) Integrated modelling of population, employment and land-use change with a multiple activity-based variable grid cellular automaton. *International Journal of Geographical Information Science*, **26**, 1251–1280.

Whitehead, P. G., Wilby, R. L., Battarbee, R. W., Kernan, M. and Wade, A. J. (2009) A review of the potential impacts of climate change on surface water quality. *Hydrological Sciences Journal*, **54**, 101–123. URL: https://doi.org/10.1623/hysj.54.1.101.

WHO (2014) *Quantitative risk assessment of the effects of climate change on selected causes of death, 2030s and 2050s*. World Health Organization.

Wilby, R. L. (2008) Constructing climate change scenarios of urban heat island intensity and air quality. *Environment and Planning B: Planning and Design*, **35**, 902–919. URL: http://epb.sagepub.com/lookup/doi/10.1068/b33066t.

Willems, P. and Vrac, M. (2011) Statistical precipitation downscaling for small-scale hydrological impact investigations of climate change. *Journal of Hydrology*, **402**, 193–205. URL: http://dx.doi.org/10.1016/j.jhydrol.2011.02.030https://linkinghub.elsevier.com/retrieve/pii/S0022169411001582.

Willett, K. M. and Sherwood, S. (2012) Exceedance of heat index thresholds for 15 regions under a warming climate using the wet-bulb globe temperature. *International Journal of Climatology*, **32**, 161–177.

Wong, N. H., Tan, C. L., Kolokotsa, D. D. and Takebayashi, H. (2021) Greenery as a mitigation and adaptation strategy to urban heat. *Nature Reviews Earth and Environment*, **2**, 166–181. URL: http://dx.doi.org/10.1038/s43017-020-00129-5.

Wouters, H., De Ridder, K., Poelmans, L., Willems, P., Brouwers, J., Hosseinzadehtalaei, P., Tabari, H., Vanden Broucke, S., van Lipzig, N. P. and Demuzere, M. (2017) Heat stress increase under climate change twice as large in cities as in rural areas: A study for a densely populated midlatitude maritime region. *Geophysical Research Letters*, **44**, 8997–9007.

Zhang, X., Liu, L., Wu, C., Chen, X., Gao, Y., Xie, S. and Zhang, B. (2020) Development of a global 30 m impervious surface map using multisource and multitemporal remote sensing datasets with the Google Earth Engine platform. *Earth System Science Data*, **12**, 1625–1648. URL: https://essd.copernicus.org/articles/12/1625/2020/.

Zhao, M., Lee, J. K. W., Kjellstrom, T. and Cai, W. (2021a) Assessment of the economic impact of heat-related labor productivity loss: a systematic review. *Climatic Change*, **167**, 22. URL: https://link.springer.com/10.1007/s10584-021-03160-7.

Zhao, Q., Guo, Y., Ye, T., Gasparrini, A., Tong, S., Overcenco, A., Urban, A., Schneider, A., Entezari, A., Vicedo-Cabrera, A. M. et al. (2021b) Global, regional, and national burden of mortality associated with non-optimal ambient temperatures from 2000 to 2019: a three-stage modelling study. *The Lancet Planetary Health*, **5**, e415–e425.

Zheng, S., Zhao, L. and Li, Q. (2016) Numerical simulation of the impact of different vegetation species on the outdoor thermal environment. *Urban forestry & urban greening*, **18**, 138–150.

Zhou, B., Lauwaet, D., Hooyberghs, H., De Ridder, K., Kropp, J. P. and Rybski, D. (2016) Assessing Seasonality in the Surface Urban Heat Island of London. *Journal of Applied Meteorology and Climatology*, **55**, 493–505. URL: https://journals.ametsoc.org/view/journals/apme/55/3/jamc-d-15-0041.1.xml.

Zhou, B., Rybski, D. and Kropp, J. P. (2017) The role of city size and urban form in the surface urban heat island. *Scientific Reports*, **7**, 4791. URL: https://www.nature.com/articles/s41598-017-04242-2.

Zhou, D., Xiao, J., Bonafoni, S., Berger, C., Deilami, K., Zhou, Y., Frolking, S., Yao, R., Qiao, Z. and Sobrino, J. A. (2019) Satellite remote sensing of surface urban heat islands: Progress, challenges, and perspectives. *Remote Sensing*, **11**, 1–36.